Fluidic Thrust Shock-Vectoring Control: A Sensitivity Analysis

Khaled Younes * and Jean-Pierre Hickey†
University of Waterloo, Waterloo, ON, N2L 3G1

Nomenclature

C_d = discharge coefficient

D_j = injector diameter (mm)

h = penetration height (mm)

l_s = separation distance (mm)

N = number of variables

N_s = sample size

NPR = nozzle pressure ratio (P_{o1}/P_∞)

P_o = total pressure (MPa)

P_p = plateau pressure (MPa)

r_e = exit radius (mm)

r_{th} = throat radius (mm)

S = Sobol indices

SPR = secondary pressure ratio (P_{oj}/P_{o1})

x_d = secondary shock location (mm)

x_m = injection location (mm)

x_s = primary shock location (mm)

x_t = length of divergent section (mm)

ϵ = total relative error

δ = deflection angle (°)

γ = ratio of specific heats (C_p/C_v)

ψ = bow shock azimuth angle (°)

Subscripts

1 = primary flow

i = iteration number

*Research Assistant, Mechanical and Mechatronics Engineering, 200 University Avenue West; kyounes@edu.uwaterloo.ca (Corresponding Author).

†Assistant Professor, Mechanical and Mechatronics Engineering, 200 University Avenue West.

j = secondary jet flow

k = arbitrary variable

T = total indices

x = axial coordinate

y = normal coordinate

I. Introduction

The recent resurgence of interest and increased accessibility to the commercial space market has driven the establishment of numerous private space companies. With it, an increased diversity in the designs of launch vehicles was brought about. The forefront of space technology is then maintained through innovative, low-cost designs with minimal complexity. One area still ripe for development is the guidance, navigation, and control (GNC) system of the booster rocket (first stage of a multistage launch vehicle). Historically, successful techniques for navigation involved "gimballing" of the rocket engine, which required mechanical actuators and pumps, a supply of hydraulic fluid, and separate hydraulic lines for activation. For light-to-medium class launch vehicles, this technique can be overly complex, heavy, and expensive.

The ability of a multistaged rocket to navigate through the upper levels of the atmosphere remains of fundamental importance. A promising alternative to mechanical steering is fluidic thrust vectoring (FTV), of which three distinct classes exist: shock-vectoring, counterflow, and throat shifting. A detailed description of each of these methods is given in [1]. In this Note, we focus solely on shock-vector control (SVC). The main premise of SVC lies in the injection of a secondary fluid in the divergent portion of a supersonic nozzle. Then, through the resulting shock wave pattern, an asymmetric distribution in wall pressure is created, yielding a deflection in the overall thrust vector. The concept is attractive for new, low-cost space vehicles because it has no moving parts, it is lightweight, and it offers fast response times [2].

In the literature, several studies have been conducted to investigate the parameters affecting SVC performance. Experimental [3–7], numerical [6, 8–11], and analytical [12–18] methods have been encompassed. To guide the designer in the preliminary stages of design however, analytical methods have proven to be particularly valuable; they allow full exploration of the parameter space without incurring significant computational or experimental costs. Out of the various analytical models (blunt-body [12–15], linear [19], and blast-wave theory [20]), the blunt-body model initially developed by Spaid [12, 15] and Zukoski [13, 14] in the 1960s for flows over two-dimensional flat plates and later extended by Maarouf [16] to cover three-dimensional nozzle flows is most robust. Despite its robustness, the model relies on empirical formulations to simplify the computation and the flow physics. It is not presently well-understood, in the context of SVC, what impacts these formulations have on the accuracy of the calculations. More importantly,

due to the highly convoluted nature of the model, it is not clear how the multitude of variables interact in any given computation. Thus, in this Note, we aim to present a sensitivity analysis to quantify the impacts of main flow variables and assumptions on the outcome of a SVC model.

II. Methodology

The low-order analytical SVC model used in this study was developed in-house based on the work of Maarouf [16]. The work of Maarouf [16] was used as basis for the derivation because it is generic and readily applicable to any three-dimensional nozzle flow and geometry. The in-house model was extensively validated against publicly available data [3, 4, 6, 7, 9–11, 16, 17], with a maximum error of 13%. The model is comprised of two main subroutines: (1) calculation of the separation distance and (2) estimation of surface forces. The first subroutine takes as input a total of 11 independent variables ($\gamma_1, \gamma_j, P_{o1}, P_{oj}, \text{NPR}, x_m, x_t, r_{th}, r_e, D_j, C_d$) and outputs h, l_s, x_s, and P_p based on the one-dimensional isentropic nozzle flow equations and oblique shock relations [21], an empirical shock criterion, and a quarter-sphere blunt-body model [12]. The second subroutine uses the characteristic length scale h (radius of solid-body quarter-sphere) to calculate ψ and an empirical free-shock separation (FSS) criterion to compute x_d and then integrates the wall pressure profile to obtain F_x and F_y. The deflection angle is calculated by

$$\delta = tan^{-1}(F_y/F_x). \tag{1}$$

A block diagram showing the algorithmic steps is given in Figure 1; the nozzle parameters are highlighted in Figure 2. A detailed overview of the model is also presented in [10].

Prior to performing the sensitivity analysis, a baseline case is selected from which the nominal values are obtained. This is chosen to be the conical nozzle geometry of Sellam *et al.* [17], where $\delta_{model} = 7.9°$ for SPR = 1. Following that, the uncertainty in the inputs is quantified, corresponding to the lower and upper bounds of the variables. The uncertainty in each variable is quantified according to: the measurement error in geometric features (± half of the measuring unit for $x_m, x_t, r_{th}, r_e, D_j$), high temperature effects in the ratio of specific heats (± 5% for $\gamma_{1,j}$), the accuracy of pressure gauges and flow meters (± 1 kPa for $P_{o1,j}$ and ± 1 % for C_d [22]), and the variability due to different separation criteria (± 6% for x_s, x_d, P_p, ψ [17]). The sensitivity analysis is then conducted by sampling the input parameters, summarized in Table 1, and analyzing the outputs using a Sobol analysis [23, 24]. Here, the sampling is done using Saltelli's [25] extension of the Sobol [23] sequence. The analysis method is a global variance-based approach where the total variance of the model output (in this case δ) is divided into contributions from each input and each set of inputs; these divisions resemble the Sobol sensitivity indices. The method is implemented as part of an open-source Python library, SALib [26].

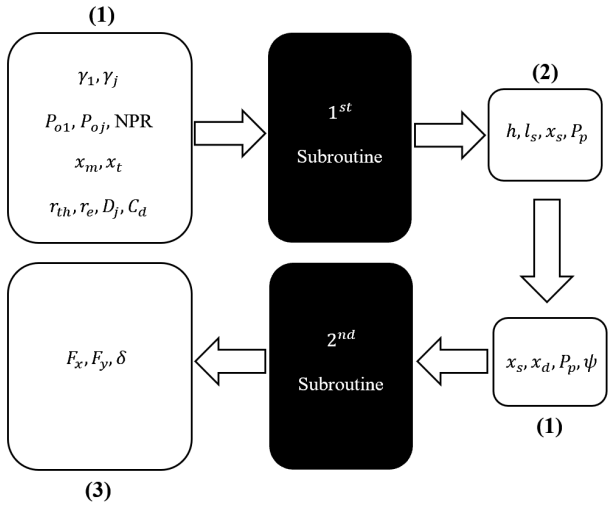

Fig. 1 Flowchart describing the execution of the SVC model. (1): inputs, (2): intermediary variables, and (3): outputs.

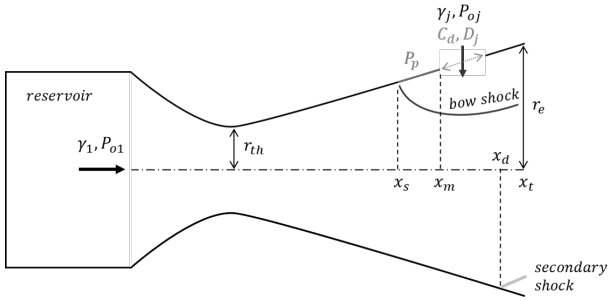

Fig. 2 Schematic diagram of the variables in SVC.

III. Results

Two sensitivity analyses are conducted at two NPR values: NPR = 37.5 (ideal case) and NPR = 15 (over-expanded case). The reason behind the selection of NPR = 15 is twofold. First, it was shown that SVC is most effective at over-expanded conditions [18]. Second, flow separation was observed inside the nozzle for highly over-expanded conditions, NPR < 15, severely deteriorating SVC performance [10]. To ensure a converged sample size N_S, the relative error in the total Sobol indices is monitored at each iteration i by summing over each variable k and weighing the result by the number of variables in the set, N. The value of the total relative error can be represented as

$$\varepsilon = \frac{1}{N}\sum_{k=1}^{N} ||S_{T,i,k} - S_{T,i-1,k}||, \tag{2}$$

where it is plotted as a function of sample size for both cases in Figure 3. Since the magnitude of the error does not notably change beyond $N_S > 128$, we select $N_S = 128$ as our sample size; this corresponds to a total of 3,840 distinct simulations. The program is run on a dual-core Intel i7 processor with a clock time of ~35 minutes.

Table 1 Range of parameters studied in the sensitivity analysis. The last column details the values used in Sellam *et al* [17].

Variable	lower bound	upper bound	nominal value [17]
1^{st} Subroutine			
γ_1	1.32	1.4	1.4
γ_j	1.32	1.4	1.4
P_{o1}	3.749	3.751	3.75
P_{oj}	3.749	3.751	3.75
x_m	85	95	90
x_t	95	105	100
r_{th}	9.67	9.77	9.72
r_e	20.08	20.18	20.13
D_j	5.95	6.05	6
C_d	0.8415	0.8585	0.85
2^{nd} Subroutine			
x_s	74.26	83.74	79
x_d	84.6	95.4	90
P_p	0.3525	0.3975	0.375
ψ	69.5	78.3	73.9

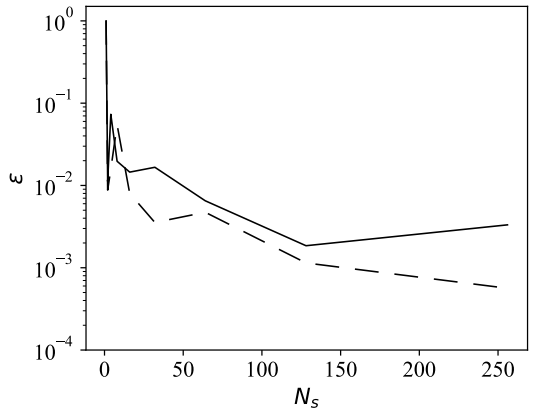

Fig. 3 Total relative error as a function of sample size for NPR = 37.5 (solid line) and NPR = 15 (dashed line).

First- and total-order Sobol indices are plotted in Figure 4 for both NPR values. While first-order indices indicate linear dependencies (i.e. how the output is affected by varying one variable alone), total-order indices, if substantially larger than first-order indices, reveal higher-order nonlinear interactions between the variables [27]. As can be seen, the interactions in the SVC model are primarily linear, with no large discrepancies observed between first- and total-order indices. Further, we observe that two primary variables are responsible for the majority of the variation in the deflection angle δ; namely, the location of the injector x_m and the primary shock x_s in the ideal case and the location of the injector x_m and the secondary shock x_d in the over-expanded case. (Note that x_d has no impact in the ideal case because no secondary shocks are expected downstream of the injection.) This establishes the notion that accurate estimation of the shock position is necessary to refine the model and that solely relying on empirical correlations may introduce erroneous errors. Currently, no such estimates exist. Additionally, a consistent and cautious approach must be taken when measuring and reporting the injector location, as small variations can lead to significant changes in the

deflection angle. It is worth mentioning that the bow shock angle ψ plays a minor role in changing the output under ideal conditions and has no impact at over-expanded conditions. This, along with the fact that the plateau pressure P_p minimally influences δ, indicates that current modelling techniques for those parameters are sufficiently resolved.

To gain more insight into the impacts of the two primary inputs outlined above, the change in δ is quantified as a function of x_m and x_s for the ideal case and x_m and x_d for the over-expanded case (Figure 5). For NPR = 37.5, we note that the maximum theoretical δ can be obtained by pushing the location of the injector towards the exit of the nozzle and increasing the separation distance l_s (thereby reducing x_s); this maximizes the area over which the highest pressure in the nozzle, P_p, acts. On the other hand, in the over-expanded case, δ can be maximized by bringing the location of the injector towards the nozzle throat and delaying the formation of the secondary shock (larger x_d). Since the secondary shock equalizes the pressure with ambient, delaying it is advantageous for increasing δ. It is important to point out that minor changes in x_d ($\pm 6\%$) yield significant changes in δ ($\Delta\delta \approx 20\%$); this further establishes the need for accurate estimation of the secondary shock position.

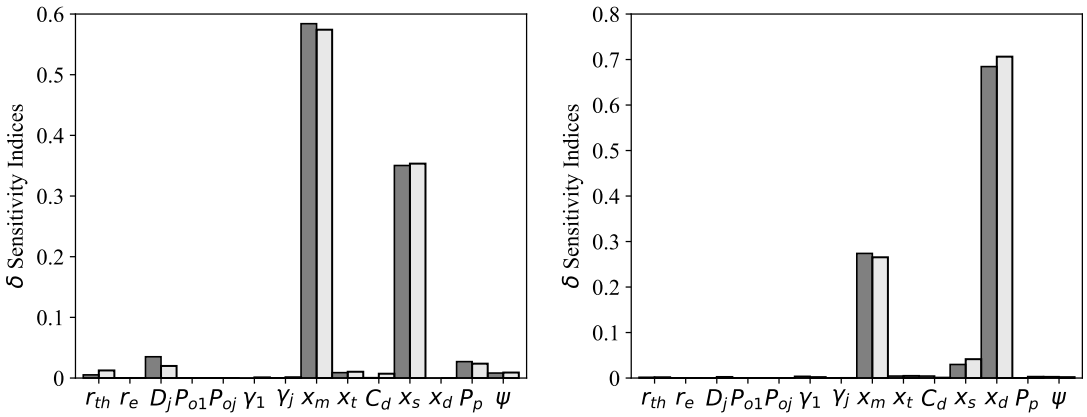

Fig. 4 First- and Total-Order sensitivity indices for δ. Dark gray bars indicate first-order indices; light gray bars represent total-order indices. Left window corresponds to the ideal case (NPR = 37.5); right window is for the over-expanded case (NPR = 15).

IV. Conclusion

Fluidic shock-vector control offers several advantages over traditional thrust vectoring methods for intermediate launch vehicles. Multiple analytical models have been devised to provide rapid predictions of shock-vector control performance. However, the interactions of flow inputs and impacts of modeling assumptions have never been presented. In this Note, a global variance-based sensitivity study is conducted to address those issues. It is shown that the model inputs interact primarily linearly with 2 prominent variables — the position of the shocks and the injector. It is also shown that current empirical correlations used for estimating the shock position require refinement. In the context of shock-vector control, a need is established for high fidelity modelling of shock locations, particularly in over-expanded

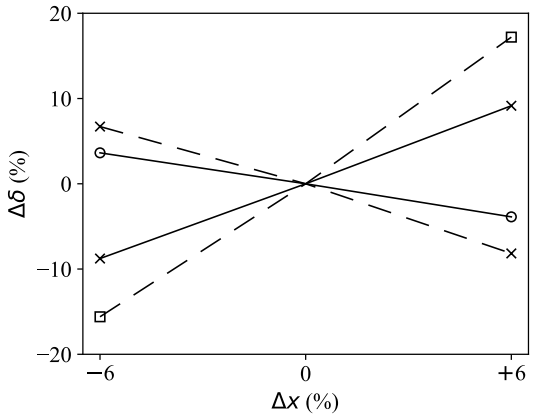

Fig. 5 Relative change in deflection angle δ due to changes in primary variables. NPR = 37.5 (solid lines) and NPR = 15 (dashed lines). (×): x_m, (○): x_s, and (□): x_d.

conditions.

Acknowledgments

This work builds on a fruitful collaboration with Reaction Dynamics Canada. We acknowledge the support of the Natural Sciences and Engineering Research Council of Canada (NSERC).

References

[1] Deere, K., "Summary of fluidic thrust vectoring research at NASA Langley Research Center," *The 21st AlAA Applied Aerodynamics Conference*, American Institute of Aeronautics and Astronautics (AIAA), Orlando, FL, 2003. doi:10.2514/6.2003-3800.

[2] Hausmann, G. F., "Thrust axis controI of supersonic nozzles by airjet shock interference," Tech. rep., United Aircraft Corporation, 1952.

[3] Masuya, G., Chinzei, N., and Ishii, S., "Secondary gas injection into a supersonic conical nozzle," *AIAA Journal*, Vol. 15, No. 3, 1977, pp. 301–302. doi:10.2514/3.63234.

[4] Wing, D. J., and Giuliana, V. J., "Fluidic thrust vectoring of an axisymmetric exhaust nozzle at static conditions," *ASME Fluids Engineering Division Summer Meeting*, American Society of Mechanical Engineers, Vancouver, BC, 1997.

[5] Anderson, C., Giuliano, V. J., and Wing, D. J., "Investigation of hybrid fluidic/mechanical thrust vectoring for fixed-exit exhaust nozzles," *33rd Joint Propulsion Conference and Exhibit*, American Institute of Aeronautics and Astronautics (AIAA), Seattle, WA, 1997. doi:10.2514/6.1997-3148.

[6] Waithe, K. A., and Deere, K. A., "An experimental and computational investigation of multiple injection ports in a convergent-divergent nozzle for fluidic thrust vectoring," *The 21st AIAA Applied Aerodynamics Conference*, American Institute of Aeronautics and Astronautics (AIAA), Orlando, FL, 2003. doi:10.2514/6.2003-3802.

[7] Sellam, M., Zmijanovic, V., Leger, L., and Chpoun, A., "Assessment of gas thermodynamic characteristics on fluidic thrust vectoring performance: analytical, experimental and numerical study," *International Journal of Heat and Fluid Flow*, Vol. 53, 2015, pp. 156–166. doi:10.1016/j.ijheatfluidflow.2015.03.005.

[8] Ko, H., and Yoon, W.-S., "Performance analysis of secondary gas injection into a conical rocket nozzle," *Journal of Propulsion and Power*, Vol. 18, No. 3, 2002, pp. 585–591. doi:10.2514/2.5972.

[9] Deng, R., Kong, F., and Kim, H. D., "Numerical simulation of fluidic thrust vectoring in an axisymmetric supersonic nozzle," *Journal of Mechanical Science and Technology*, Vol. 28, No. 12, 2014, pp. 4979–4987. doi:10.1007/s12206-014-1119-x.

[10] Zmijanovic, V., Lago, V., Sellam, M., and Chpoun, A., "Thrust shock vector control of an axisymmetric conical supersonic nozzle via secondary transverse gas injection," *Shock Waves*, Vol. 24, No. 1, 2014, pp. 97–111. doi:10.1007/s00193-013-0479-y.

[11] Li, L., Hirota, M., Ouchi, K., and Saito, T., "Evaluation of fluidic thrust vectoring nozzle via thrust pitching angle and thrust pitching moment," *Shock Waves*, Vol. 27, No. 1, 2017, pp. 53–61. doi:10.1007/s00193-016-0637-0.

[12] Spaid, F. W., "A study of secondary injection of gases into a supersonic flow," Ph.D. thesis, California Institute of Technology, 1964.

[13] Zukoski, E. E., and Spaid, F. W., "Secondary injection of gases into a supersonic flow," *AIAA Journal*, Vol. 2, No. 10, 1964, pp. 1689–1696. doi:10.2514/3.2653.

[14] Zukoski, E. E., "Turbulent boundary-layer separation in front of a forward-facing step," *AIAA Journal*, Vol. 5, No. 10, 1967, pp. 1746–1753. doi:10.2514/3.4299.

[15] Spaid, F. W., and Zukoski, E. E., "A study of the interaction of gaseous jets from transverse slots with supersonic external flows," *AIAA Journal*, Vol. 6, No. 2, 1968, pp. 205–212. doi:10.2514/3.4479.

[16] Maarouf, N., "Modélisation des phénomènes dissymétriques dans le divergent des tuyères supersoniques propulsives: application a la vectorisation de la poussée," Ph.D. thesis, University of Évry Val d'Essonne, 2008.

[17] Sellam, M., Chpoun, A., Zmijanovic, V., and Lago, V., "Fluidic thrust vectoring of an axisymmetrical nozzle: an analytical model," *International Journal of Aerodynamics*, Vol. 2, No. 2/3/4, 2012, pp. 193–209. doi:10.1504/ijad.2012.049112.

[18] Zmijanovic, V., Lago, V., Leger, L., Depussay, E., Sellam, M., and Chpoun, A., "Thrust vectoring effects of a transverse gas injection into a supersonic cross flow of an axisymmetric convergent-divergent nozzle," *Progress in Propulsion Physics*, Vol. 4, 2013, pp. 227–256. doi:10.1051/eucass/201304227.

[19] Walker, R. E., and Shandor, M., "Influence of injectant properties for fluid-injection thrust vector control," *Journal of Spacecraft and Rockets*, Vol. 1, No. 4, 1964, pp. 409–413. doi:10.2514/3.27670.

[20] Broadwell, J. E., "Analysis of the fluid mechanics of secondary injection for thrust vector control," *AIAA Journal*, Vol. 1, No. 5, 1963, pp. 580–585. doi:10.2514/3.1726.

[21] Anderson, J. D., *Modern Compressible Flow: With Historical Perspective*, 2nd ed., McGraw-Hill, New York, 1990.

[22] Zmijanovic, V., "Secondary injection fluidic thrust vectoring of an axisymmetric supersonic nozzle," Ph.D. thesis, University of Orléans, 2013.

[23] Sobol, I. M., "Global sensitivity indices for nonlinear mathematical models and their Monte Carlo estimates," *Mathematics and Computers in Simulation*, Vol. 55, No. 1-3, 2001, pp. 271–280. doi:10.1016/S0378-4754(00)00270-6.

[24] Saltelli, A., Annoni, P., Azzini, I., Campolongo, F., Ratto, M., and Tarantola, S., "Variance based sensitivity analysis of model output. Design and estimator for the total sensitivity index," *Computer Physics Communications*, Vol. 181, No. 2, 2010, pp. 259–270. doi:10.1016/j.cpc.2009.09.018.

[25] Saltelli, A., "Making best use of model evaluations to compute sensitivity indices," *Computer Physics Communications*, Vol. 145, No. 2, 2002, pp. 280–297. doi:10.1016/S0010-4655(02)00280-1.

[26] Herman, J., and Usher, W., "An open-source Python library for sensitivity analysis," *Journal of Open Source Software*, Vol. 2, No. 9, 2017, p. 97. doi:10.21105/joss.00097.

[27] Homma, T., and Saltelli, A., "Importance measures in global sensitivity analysis of nonlinear models," *Reliability Engineering and System Safety*, Vol. 52, 1996, pp. 1–17. doi:10.1016/0951-8320(96)00002-6.